Inorganic Chemistry

Article

pubs.acs.org/IC

Relativistic and Solvation Effects on the Stability of Gold(III) Halides in Aqueous Solution

Kolja Theilacker,[†] H. Bernhard Schlegel,*[,‡] Martin Kaupp,*[,†] and Peter Schwerdtfeger*[,§]

[†]Technische Universität Berlin, Institut für Chemie, Theoretische Chemie, Sekr. C7, Straße des 17. Juni 135, 10623 Berlin, Germany

[‡]Department of Chemistry, Wayne State University, 5101 Cass Av., Detroit, Michigan 48202-3489, United States

[§]New Zealand Institute for Advanced Study, Massey University Auckland, Private Bag 102 904, North Shore MSC, 0745 Auckland, New Zealand

Supporting Information

ABSTRACT: The redox stability of gold halide complexes in aqueous solution has been examined quantum-chemically by a systematic comparison of scalar- and nonrelativistic pseudopotential calculations, using both COSMO and D-COSMO-RS solvent models for water. After a computational benchmarking of density-functional methods against CCSD(T) results for the gas phase decomposition $AuX_4^- \rightarrow AuX_2^- + X_2$, B3LYP calculations have been used to establish solvent contributions. While relativity clearly enhances the stability of AuX_4^- (X = F, Cl, Br, I) complexes against X_2 elimination, solvation favors the lower oxidation state. Solvation and relativity are nonadditive, due to the relativistic reduction of bond polarity. At scalar relativistic D-COSMO-RS level, the reaction $AuX_4^- \rightleftharpoons AuX_2^- + X_2$ is computed to be endergonic, except for X = I, where it is slightly exergonic. Under the chosen conditions, partial hydrolysis of $AuCl_4^-$ to $AuCl_3OH^-$ is exergonic. The latter complex in turn is stable against Cl_2 elimination. The disproportionation $3\ AuCl_2^- \rightleftharpoons AuCl_4^- + 2\ Au_{(s)} + 2\ Cl^-$ is clearly exergonic. All of the computed reaction energies at scalar relativistic D-COSMO-RS level agree well with the observed speciation in dilute pH-neutral solutions at ambient temperatures.

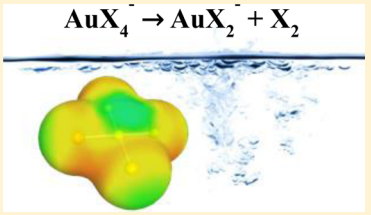

1. INTRODUCTION

The important role of relativistic effects in the chemical and physical properties of heavy-element compounds is now well established,[1−3] and the stability of oxidation states in such compounds is also a well-documented field where relativistic effects may be crucial.[4−8] A recent spectacular example is the computational proof that the lead battery is of practical use (compared to the corresponding tin cell) only because of the destabilization of the highest-oxidation-state Pb^{IV} species by scalar relativistic effects.[9] The destabilization of the highest oxidation state by relativity is a general observation in p-block main-group chemistry, leading to an enhancement of the well-known inert-pair effect. The relativistic contributions in this case are largely due to the relativistic contraction of the 6s orbitals, which renders the hybridization between 6s and 6p orbitals particularly unfavorable, enhancing so-called hybridization defects.[10−12] In contrast, relativity stabilizes the highest oxidation states of the 5d elements. This is partly due to the relativistic expansion of the 5d orbitals and the associated improved covalent bonding and better transfer of charge from metal to ligands. In the spectacular case of the stability of oxidation state + IV in mercury chemistry in form of HgF_4[6,13,14] (and the related predicted stability of the heavy homologue CnF_4[15]), it has been shown that destabilization of the lower + II oxidation state by contraction of the 6s orbitals is even more important. These works have been preceded by computational studies by one of us on the relativistic stabilization of oxidation state + III in gold chemistry about 25 years ago.[7,8] Gas-phase calculations on gold(III) halides carried out at the time showed clearly how equilibria like $AuX_3 \rightleftharpoons AuX + X_2$ are shifted to the left by scalar relativistic effects (see also ref 16.).

While such calculations show the principal stabilization of Au^{III} by relativity, the more chemically relevant processes involve gold(III) compounds in solution. In particular, the aqueous $AuCl_4^-$ anion is an important constituent in the industrial electrochemical refinement of gold in a hydrochloric acid ($HAuCl_4$) solution (Wohlwill process), in the extraction of gold by chlorine in hydrochloric acid, in the dissolution of elemental gold by aqua regia, or in certain oxidation reactions in organic synthesis.[17] The influence of relativity on the redox stability of this and similar species in aqueous solution is thus a practically important question but has hitherto not been addressed by quantum-chemical studies. The computational modeling in this case is complicated by the need to include the hydrogen bonding from the aqueous solvent with the species involved in the chemical equilibria. Moreover, the interplay between solvation and relativistic effects has not been addressed previously in the literature. In the present study we therefore use a comparison between state-of-the-art relativistic and nonrelativistic quantum-chemical methodology in combination with the Direct Conductor-like Screening Model for Real Solvents (D-COSMO-RS)[18] to address the stability of gold halide complexes AuX_4^- (X = F, Cl, Br, I) in aqueous solution against reductive elimination of halogen.

Received: July 21, 2015
Published: September 30, 2015

DOI: 10.1021/acs.inorgchem.5b01632
Inorg. Chem. 2015, 54, 9869−9875

2. COMPUTATIONAL DETAILS

Initial gas-phase calculations for the decomposition reaction $AuX_4^- \rightarrow AuX_2^- + X_2$ (X = F, Cl, Br and I) were carried out in order to select a suitable exchange-correlation functional from density functional theory (DFT) to be further applied to reactions in solution. To this end, benchmark calculations at post-Hartree−Fock coupled-cluster levels (CCSD and CCSD(T)), as well as at the Møller−Plesset MP2, MP3, MP4(SDQ) levels, were carried out with the Gaussian09 program.[19] The influence of relativistic effects has been computed by comparison of scalar-relativistically and nonrelativistically adjusted energy-consistent effective core potentials (ECPs)[20] for gold, bromine, and iodine,[21−23] while disregarding the much less important relativistic contributions from the lighter halogen atoms. Against the obtained CCSD(T) benchmark data, a range of density functionals has been screened for the relativistic and nonrelativistic gas-phase energetics, including "pure" functionals within the generalized gradient approximation (GGA) such as PW91 and PBE, the popular global hybrid B3LYP,[24] which has been previously shown to perform well for the stability of high oxidation states in transition-metal chemistry,[24−34] and finally the range-separated hybrids CAM-B3LYP[35] and LC-ωPBE.[36] The basis sets used were an uncontracted relativistic MP2 optimized (10s10p6d3f) set for gold (see Supporting Information for details), and aug-cc-pVTZ basis sets for the halides.[23,37,38]

Solvent effects were subsequently evaluated at B3LYP level with the TURBOMOLE6.3 package,[39−41] using both the COSMO and D-COSMO-RS models. These calculations have been performed using the same ECPs and basis sets as for the gas-phase calculations, performing full-structure optimizations at all levels. We note in passing that the definition of the VWN correlation functional occurring in this case is slightly different from the definition in Gaussian (VWN5 instead of VWN3[42]). As a dielectric continuum solvent model, in this case the COSMO (Conductor-like Screening Model[43]) approach was employed, using dielectric constant ε = 78.3553 for water. To go beyond a continuum model, which does not capture hydrogen bonding, the self-consistent D-COSMO-RS method[18,44] was used. This is the self-consistent variant of Klamt's COSMO-RS approach.[45,46] It is based on a statistical thermodynamics ansatz with respect to the surface charge densities of the COSMO model and incorporates explicitly terms for hydrogen bonding, thus providing a much better description for protic solvents than standard polarizable continuum models. Recent thermochemical applications of the self-consistent D-COSMO-RS implementation include organic electron-transfer[18,47] and Diels−Alder[48] reactions. The required σ-potentials have been created with the COSMOtherm program[49] at BP86/TZVP level[50] for 298 K. Self-consistent COSMO and D-COSMO-RS surface charge densities have been plotted using the same program. In the COSMO and D-COSMO-RS solvent environments, the frequency calculations had to be done by numerical differentiation of analytical gradients (using the numforce module of TURBOMOLE6.3). The computed vibrational frequencies were subsequently used to estimate thermal and entropic contributions to the Gibbs free energies of reaction.

Spin−orbit contributions to the reaction energies of the bromide and iodide complexes have been estimated by gas-phase two-component ECP calculations[51,52] with TURBOMOLE6.3 (B3LYP/dhf-QZVP-2c level[22,23] with corresponding dhf-QZVP-2c RI-JK auxiliary basis sets[53]). Two-component ECPs and valence basis sets for gold, bromine and iodine[22,23] have been used, and SO energies were obtained by taking energy differences between two-component and scalar relativistic ECP energies (as single points on scalar-relativistically optimized structures).

3. RESULTS

3.1. Gas-Phase Reaction $AuX_4^- \rightleftharpoons AuX_2^- + X_2$. As a background for the discussion of solvent effects and to validate the use of computationally more efficient DFT methods, we first compare a number of DFT functionals against benchmark coupled-cluster calculations for the gas-phase reaction of the halide systems, and we evaluate the magnitude of relativistic effects in the absence of any solvent. Tables 1 and 2 provide nonrelativistic and (scalar) relativistic ECP calculations at various computational levels for X = F, Cl and X = Br, I, respectively. Taking the CCSD(T) data as reference values, and starting with the ab initio methods, we see that the importance of electron correlation [measured by the difference between HF and CCSD(T)] is dramatically reduced at the relativistic level. Therefore, deviations of the different electron-correlation methods from the benchmark data, and the importance of the triple excitations at coupled-cluster level, are also substantially diminished by relativity. This is not unexpected, as the relativistic expansion of the Au 5d-orbitals improves the overlap with the ligand orbitals in the Au(III) species and reduces the "stretched-bond situation" typical for transition-metal complexes, in particular in high oxidation states. Partly stretched bonds, due to Pauli repulsion between 5s and 5p semicore−shells with the bonding orbitals, are responsible for the large nondynamical correlation effects found at the nonrelativistic level, while the relativistic expansion of the 5d orbitals improves the overlap and strengthens the bonds.[54,55]

Table 1. Computed Nonrelativistic and Scalar-Relativistic Gas-Phase Reaction Energies for $AuX_4^- \rightarrow AuX_2^- + X_2$ (X = F, Cl) at Various Levels and Their Deviations from CCSD(T) Data[a]

	nonrelativistic		scalar relativistic	
X = F	ΔE	deviation from CCSD(T) (kJ mol^{-1})	ΔE	deviation from CCSD(T) (kJ mol^{-1})
HF	159.4	−116.7	392.9	−16.6
MP2	291.3	15.2	404.8	−4.7
MP2//CCSD(T)	292.0	15.9	405.6	−3.9
MP3//CCSD(T)	244.6	−31.5	401.6	−7.9
MP4SDQ//CCSD(T)	261.4	−14.7	408.8	−0.7
CCSD//CCSD(T)	251.8	−24.3	404.4	−5.1
CCSD(T)	276.1		409.5	
LC-ωPBE	288.5	12.4	428.9	19.4
CAM-B3LYP	293.8	17.7	418.2	8.7
B3LYP	295.4	19.3	399.2	−10.3
PBE	333.3	57.2	409.1	−0.4
PW91	338.4	62.3	413.9	4.4
	nonrelativistic		scalar relativistic	
X = Cl	ΔE	deviation from CCSD(T) (kJ mol^{-1})	ΔE	deviation from CCSD(T) (kJ mol^{-1})
HF	−142.3	−174.5	57.5	−91.7
MP2	75.6	43.4	171.2	22.0
MP2//CCSD(T)	76.5	44.3	172.2	23.0
MP3//CCSD(T)	−2.0	−34.2	123.6	−25.6
MP4SDQ//CCSD(T)	−1.1	−33.3	134.5	−14.7
CCSD//CCSD(T)	−4.6	−36.8	127.9	−21.3
CCSDT(T)	32.2		149.2	
LC-ωPBE	9.8	−22.4	141.5	−7.7
CAM-B3LYP	21.5	−10.7	130.8	−18.4
B3LYP	40.1	7.9	126.7	−22.5
PBE	88.0	55.8	157.3	8.1
PW91	91.5	59.3	160.1	10.9

[a]For fully optimized structures at the given computational level, unless indicated otherwise.

DOI: 10.1021/acs.inorgchem.5b01632
Inorg. Chem. 2015, 54, 9869−9875

Table 2. Computed Nonrelativistic and Scalar-Relativistic Gas-Phase Reaction Energies for $AuX_4^- \rightarrow AuX_2^- + X_2$ (X = Br, I) at various Levels and Their Deviations from CCSD(T) Data[a]

	nonrelativistic		scalar relativistic	
X = Br	ΔE	deviation from CCSD(T) (kJ mol^{-1})	ΔE	deviation from CCSD(T) (kJ mol^{-1})
HF	−171.7	−183.4	0.6	−115.8
MP2	66.2	54.5	155.8	39.4
MP2//CCSD(T)	67.0	55.3	156.9	40.5
MP3//CCSD(T)	−25.7	−37.4	82.2	−34.2
MP4SDQ//CCSD(T)	−19.9	−31.6	103.2	−13.2
CCSD//CCSD(T)	−25.2	−36.9	92.6	−23.8
CCSD(T)	11.7		116.4	
LC-ωPBE	−22.1	−33.8	93.4	−23.0
CAM-B3LYP	−10.1	−21.8	83.0	−33.4
B3LYP	10.2	−1.5	82.2	−34.2
PBE	58.0	46.3	116.1	−0.3
PW91	61.5	49.8	119.1	2.7
	nonrelativistic		scalar relativistic	
X = I	ΔE	deviation from CCSD(T) (kJ mol^{-1})	ΔE	deviation from CCSD(T) (kJ mol^{-1})
HF	−197.4	−193.1	−61.4	−138.9
MP2	56.3	60.6	133.8	56.3
MP2//CCSD(T)	56.1	60.4	134.4	56.9
MP3//CCSD(T)	−45.5	−41.2	33.2	−44.3
MP4SDQ//CCSD(T)	−33.3	−29.0	65.9	−11.6
CCSD//CCSD(T)	−42.2	−37.9	50.1	−27.4
CCSDT(T)	−4.3		77.5	
LC-ωPBE	−57.1	−52.8	45.5	−32.0
CAM-B3LYP	−47.2	−42.9	32.1	−45.4
B3LYP	−25.0	−20.7	34.5	−43.0
PBE	22.3	18.0	73.3	−4.2
PW91	25.9	21.6	76.3	−1.2

[a]For fully optimized structures at the given computational level, unless indicated otherwise.

Notably, the d-orbital participation in bonding in the AuX_2^- reductive elimination product is much smaller (see below), which is why the correlation effects are much less critical on the product than on the educt side of the reaction. Such considerations have been discussed previously, e.g. for the reaction $HgF_4 \rightleftharpoons HgF_2 + F_2$, or for other redox reactions in transition-metal chemistry.[14] We note in passing that the Møller−Plesset perturbation series shows the oscillatory behavior expected for such a situation, with the MP4SDQ data being somewhat closer to CCSD(T) than to CCSD.[8] Furthermore, differences between MP2 and CCSD(T) structures influence the computed MP2 reaction energies by less than 2 kJ mol^{-1}.

As these correlation contributions stabilize Au(III) relative to Au(I), the CCSD(T) reaction energies are more positive compared to the HF data, albeit the effects are much less dramatic once scalar relativity has been included (Table 1). At the CCSD(T) reference level, scalar relativity stabilizes AuX_4^- with respect to reductive elimination of X_2 by between 133.4 kJ mol^{-1} (X = F) and 81.8 kJ mol^{-1} (X = I).

As expected, the effect decreases with decreasing electronegativity of the halogen. This is related mainly to the scalar relativistic destabilization of the Au−X bonds in the Au^{I} species, where the relativistic contraction of the Au 6s orbital reduces substantially the bond ionicity and the associated electrostatic stabilization.[15] As this destabilizing effect is most pronounced with the most electronegative ligands, the decrease of the relativistic stabilization of Au(III) against Au(I) from X = F toward X = I is understandable.

These gas-phase data can now be used to judge the performance of DFT methods. The PW91 and PBE GGA functionals show excellent agreement with the reference data at the scalar relativistic level but overestimate the stability of the Au(III) complexes appreciably at the nonrelativistic level. They thus do not provide a very accurate account of the overall relativistic contributions, overestimating them by up to 60 kJ mol^{-1} (Table 1). The B3LYP global hybrid and the CAM-B3LYP and LC-ωPBE range-separated hybrids show a somewhat more uniform behavior and thus seem better suited to discuss relativistic effects. While the range hybrids perform more consistently overall, the deviations of the B3LYP data from the CCSD(T) reference are sufficiently small (smaller than or comparable to those of the CCSD values). We may therefore, in the following, use with confidence the B3LYP functional for the evaluation of solvent effects. We note that other functionals may well perform better than the ones tested here, but an exhaustive evaluation is beyond the scope of the present work.

We note in passing that spin−orbit (SO) effects on the gas-phase reactions turn out to be minor: at two-component ECP level (B3LYP, gas phase), spin−orbit contributions to the reaction energies of the bromide and iodide complexes are only about +5 kJ mol^{-1} (Table S2, Supporting Information). While the absolute SO effects stemming from iodine are, as expected, larger than for bromine, the differential effects on the reaction energy are almost the same, and the very small halogen SO contributions even cancel part of the also small gold SO contributions for these closed-shell reactions (Table S2). SO effects are therefore only marginally involved in the trend of decreasing reaction energies with heavier halide ligands, which is largely due to the decreasing ligand electronegativity (see above). We also conclude that we may, to a good approximation, discuss the reaction energies in solution at the scalar relativistic level.

3.2. $AuX_4^- \rightleftharpoons AuX_2^- + X_2$ (X = F, Cl, Br, I) Reaction in Aqueous Solution: Relativistic and Solvation Effects at the B3LYP Level. As we move to the solution phase, our focus will be on Gibbs free reaction energies rather than taking solely electronic energy differences. The solvent models cover solvent enthalpic and entropic contributions, and it is thus more consistent to include those as well for the internal degrees of freedom. The Gibbs free energies are in any case the decisive thermochemical measure determining the equilibrium. We will concentrate on the interplay between relativistic and solvent effects. It is important to note that the data provided pertain to 298 K and to neutral pH (Table 3). For the chloride species, it is well-known that both pH and temperature affect the speciation in solution appreciably, a point we will address further below. Furthermore, we may need to include other reactions than halogen elimination (e.g., disproportionation of $AuCl_2$), which we will also do below. We also note that the behavior of AuF_4^- deviates from that of the other three Au(III) halides by exhibiting a strongly endergonic elimination reaction already at nonrelativistic level, due to the inherent instability of F_2 (Table 3).

DOI: 10.1021/acs.inorgchem.5b01632
Inorg. Chem. 2015, 54, 9869−9875

Table 3. Reaction Energies, Enthalpies, And Gibbs Free Energies (in kJ mol^{-1}) for the $AuX_4^- \rightarrow AuX_2^- + X_2$ Reaction (X = F, Cl, Br, I), Together with NPA Charges and Au-X Distances (in Å) of Educt AuX_4^- (e) and Product AuX_2^- (p)[a]

reaction	nonrelativistic						relativistic					
	ΔE	$\Delta G_{298\ K}$	$\Delta H_{298\ K}$	q (Au)$_e$	q (X)$_e$	d (Au-X)$_e$	ΔE	$\Delta G_{298\ K}$	$\Delta H_{298\ K}$	q (Au)$_e$	q (X)$_e$	d (Au-X)$_e$
				q (Au)$_p$	q (X)$_p$	d (Au-X)$_p$				q (Au)$_p$	q (X)$_p$	d (Au-X)$_p$
X = F												
gas phase	295.4	254.9	292.8	1.60	−0.65	2.008	399.2	359.8	396.4	1.57	−0.64	1.941
				0.76	−0.88	2.160				0.53	−0.76	1.990
COSMO	256.6	214.4	253.9	1.64	−0.66	2.007	378.3	339.1	375.5	1.60	−0.65	1.939
				0.83	−0.91	2.199				0.55	−0.77	1.990
D-COSMO-RS	200.2	156.1	197.6	1.70	−0.67	2.012	359.5	320.0	356.8	1.64	−0.66	1.941
				0.90	−0.95	2.289				0.62	−0.81	2.017
X = Cl												
gas phase	40.1	2.3	37.7	1.09	−0.52	2.428	126.7	88.7	124.2	0.96	−0.49	2.335
				0.66	−0.83	2.505				0.37	−0.68	2.322
COSMO	4.4	−34.8	1.9	1.10	−0.53	2.424	100.9	62.7	98.3	0.97	−0.49	2.331
				0.72	−0.86	2.525				0.37	−0.68	2.314
D-COSMO-RS	−29.5	−68.5	−31.9	1.11	−0.53	2.426	91.2	52.8	88.6	0.97	−0.49	2.332
				0.80	−0.90	2.566				0.40	−0.70	2.322
X = Br												
gas phase	10.2	−26.2	7.7	0.93	−0.48	2.588	82.2	44.9	79.6	0.77	−0.44	2.488
				0.62	−0.81	2.632				0.31	−0.65	2.452
COSMO	−23.0	−61.0	−25.5	0.95	−0.49	2.583	55.8	18.5	53.3	0.77	−0.44	2.484
				0.67	−0.83	2.649				0.29	−0.65	2.442
D-COSMO-RS	−42.9	−82.2	−45.5	0.95	−0.49	2.584	50.7	13.3	48.1	0.77	−0.44	2.484
				0.73	−0.87	2.699				0.31	−0.66	2.444
X = I												
gas phase	−25.0	−59.8	−27.5	0.72	−0.43	2.813	34.5	−1.5	31.9	0.53	−0.38	2.697
				0.54	−0.77	2.800				0.22	−0.61	2.621
COSMO	−55.4	−91.3	−58.0	0.73	−0.43	2.808	7.8	−28.3	5.2	0.52	−0.38	2.693
				0.58	−0.79	2.808				0.19	−0.60	2.611
D-COSMO-RS	−64.4	−100.1	−67.0	0.72	−0.43	2.808	7.2	−29.6	4.6	0.52	−0.38	2.693
				0.60	−0.80	2.816				0.20	−0.60	2.617

[a]Comparison of gas-phase and aqueous solution results (with COSMO and D-COSMO-RS) at B3LYP level with Turbomole, using a nonrelativistic or scalar relativistic Au ECP, respectively.

In general, solvent effects are larger at the D-COSMO-RS compared to the COSMO level of theory, consistent with the lack of explicit hydrogen-bonding terms in the COSMO dielectric continuum model. The consequently larger reduction of the gas-phase Gibbs free energies of reaction at D-COSMO-RS level is expected to be more realistic, as has been shown recently for organic reactions in aqueous[48] or alcoholic solution,[18,47] and in the following, we will concentrate on these. Solvent and relativistic effects on ΔG are clearly nonadditive (Figure 1): while the reduction of ΔG from gas phase to D-COSMO-RS ranges from −99 kJ mol^{-1} (X = F) to −40 kJ mol^{-1} (X = I) at nonrelativistic levels, it is much smaller upon inclusion of scalar relativistic effects, between −40 kJ mol^{-1} (X = F) and −28 kJ mol^{-1} (X = I). In both cases, however, the solvent contributions become less negative from X = F to X = I (Figure 1, Table 3). As a result of the smaller reduction of the Gibbs free energy of reaction by solvent effects at the relativistic level, the overall relativistic stabilization of the Au(III) complexes against reductive elimination by relativity is enhanced in solution compared to the gas phase. This "extra relativistic effect by solvation" is most pronounced for X = F (+59 kJ mol^{-1}) and decreasing (from +35 kJ mol^{-1} for Cl to +12 kJ mol^{-1} for I) for the other halides.

While at nonrelativistic levels only the Au(III) fluoride complex would be stable with respect to reductive elimination, the final scalar relativistic Gibbs free reaction energies in solution (D-COSMO-RS data; Table 3) are even larger for X = F, still appreciably positive for X = Cl, less positive for X = Br, and negative for X = I (while the gas-phase reaction would be predicted to be almost thermoneutral at this level; Table 3). These results are consistent with the observation of $AuCl_4^-$ and

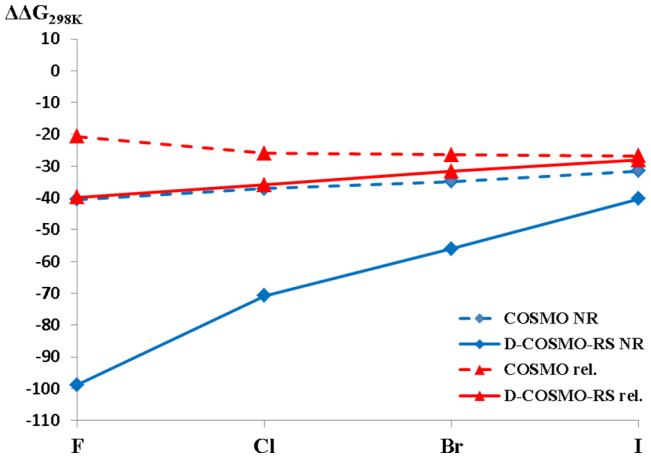

Figure 1. Differential solvent effects on Gibbs free energies, $\Delta\Delta G = \Delta G(aq) - \Delta G(g)$, at standard conditions for reaction $AuX_4^- \rightarrow AuX_2^- + X_2$ (X = F, Cl, Br, I), at COSMO and D-COSMO-RS levels (B3LYP).

DOI: 10.1021/acs.inorgchem.5b01632
Inorg. Chem. 2015, 54, 9869−9875

$AuBr_4^-$ in aqueous solution[17] and the known instability of the iodide complex under the same conditions. The fact that AuF_4^- exists only in water-free environments is due to its sensitivity to hydrolysis rather than to its oxidation power.

3.3. Interpretation of Trends in Solvent and Relativistic Effects. It is important to rationalize why (a) relativistic effects stabilize, (b) solvent effects destabilize the Au(III) oxidation state, and (c) the solvent destabilization is much less pronounced at relativistic than at nonrelativistic levels (nonadditivity of solvent and relativistic effects). Point a has been discussed in detail in previous work,[7] and we thus only summarize the salient features here: the relativistic stabilization of the Au-X bonds in the Au(III) halides due to the relativistic expansion of the 5d orbitals and the ensuing improved bonding in the higher oxidation state dominate. The destabilization of the Au(I) halides by the relativistic contraction of the 6s-orbital provides an additional, smaller driving force in favor of the higher oxidation state.

Point b, that is, the fact that solvent effects destabilize the higher oxidation state is in keeping with previous studies on, for example, mercury fluorides regarding environmental effects on the relative stability of different oxidation states. For example, it has been shown that aggregation of HgF_2 in the solid state disfavors the formation of HgF_4.[56] The reason is the larger M−X bond polarity of the halides in the lower oxidation state, in the present case AuX_2^- compared to AuX_4^-. This is obvious from the halogen natural population analysis (NPA) charges in Table 3, which generally have more negative values for the Au(I) than for the Au(III) complex. Solvation enhances the negative halogen charge (and thus the bond polarity) further, again in particular for the Au(I) complexes, and in particular at the nonrelativistic level. Due to the larger interactions for the more ionic Au(I) halides, this leads to a destabilization of the Au(III) state, most pronouncedly so for the fluoride. However, as the relativistic contraction of the 6s orbital reduces substantially the bond polarity in the Au(I) halides and far less for the Au(III) halides (due to the 5d orbital involvement in bonding), the differences in halogen charges between Au(I) and Au(III) complex are diminished considerably at the scalar relativistic level (Table 3). Therefore, the ability of the solvent effects to destabilize the Au(III) oxidation state relative to the Au(I) state is reduced appreciably by relativity. This explains the nonadditivity of solvent and relativistic effects, point c.

We note further that all of these observations are more pronounced for D-COSMO-RS than for COSMO, in line with the additional effect of hydrogen bonding beyond the bulk solvent contribution. Figure 2 provides a further illustration of these considerations by plotting surface charge densities for all species studied, comparing COSMO and D-COSMO-RS results for X = Cl. It is clear that the charge densities around the chlorine atoms are much more negative for $AuCl_2^-$ compared to $AuCl_4^-$, and that this difference is far less pronounced at the scalar relativistic than at the nonrelativistic level. Moreover, the COSMO and D-COSMO-RS surface charge densities for $AuCl_2^-$ show the most pronounced differences as well: at the nonrelativistic level, the main effect of D-COSMO-RS over COSMO is a more negative surface charge density along the molecular axis, corresponding to a less pronounced "σ-hole". In contrast, at the scalar relativistic level, D-COSMO-RS enhances the surface charge density cylindrically around the chlorine atoms, whereas the σ-hole is even enhanced slightly. Moreover, the surface charge densities around the gold center are increased (they become positive)

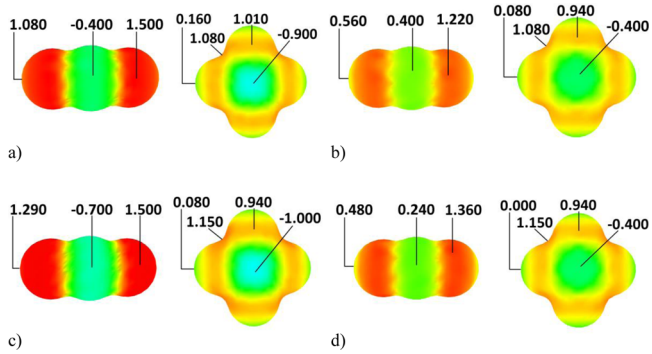

Figure 2. COSMO and D-COSMO-RS surface charge density plots for $AuCl_2^-$ and $AuCl_4^-$. Numbers for areas with maximum or minimum surface charges (in e/nm^2). (a) COSMO nonrelativistic, (b) COSMO scalar relativistic, (c) D-COSMO-RS nonrelativistic, (d) D-COSMO-RS scalar relativistic.

by relativity, and they are decreased (they become more negative or less positive) at D-COSMO-RS compared to COSMO level (note that the surface charge densities are those induced by the solute at the surface of the COSMO cavity, i.e., the signs are complementary to, e.g., the atomic charges).

3.4. On the Hydrolysis of $AuCl_4^-$. Speciation of gold chlorides in aqueous solution is of substantial geochemical importance, for example, in the context of Au transport, deposition, and concentration.[57] While $AuCl_4^-$ clearly dominates in acidic chloride solutions (with reduction to $AuCl_2^-$ occurring only at hydrothermal temperatures),[58] hydrolysis is known to play an increasing role at higher pH values.[59] Resonance Raman spectroscopy of dilute solutions at room temperature has indicated that $AuCl_4^-$ is the dominant species below pH = 5; at pH = 5.8, $AuCl_3OH^-$ starts to form, becomes about equally important as $AuCl_4^-$ at pH = 6.2, and should dominate near pH = 7. At still higher pH values, further hydrolysis takes place, and at pH > 10, $AuCl(OH)_3^-$ is the dominant species. EXAFS spectroscopy also suggests that $AuCl_3OH^-$ is the dominant species between pH = 7.5 and 9.2.[60]

As our D-COSMO-RS calculations should most closely approximate the situation in dilute solution near neutral pH and ambient temperatures, we have computed the reaction energies for $AuCl_4^- + OH^- \rightleftharpoons AuCl_3OH^- + Cl^-$ (Table 4). The results clearly show that both in the gas phase and for the solvent models used, the equilibrium is on the right-hand side. Solvation stabilizes $AuCl_4^-$ more than $AuCl_3OH^-$ and thus renders the reaction less exergonic. This effect is more pronounced with the more realistic D-COSMO-RS than with COSMO (Table 4). Relativity enhances the exergonicity slightly (by ca. 13 kJ/mol at D-COSMO-RS level). Most of this relativistic increase (9.3 kJ mol^{-1}) is already present in the gas phase, suggesting a largely intramolecular origin. Indeed, gold NPA charges in $AuCl_4^-$ are relativistically reduced from 1.11 (1.09) to 0.97 (0.96) at the D-COSMO-RS (gas phase) level, and those in $AuCl_3OH^-$ from 1.21 (1.19) to 1.10 (1.09). These charges point to an overall more polar bonding and to a smaller relativistic loss of ionic contributions to the binding energy in the hydroxo complex.

In view of the likely predominance of $AuCl_3OH^-$ under the chosen conditions, it is also of interest to examine its redox stability (Table 4): the redox reaction $AuCl_3OH^- \rightleftharpoons AuClOH^- + Cl_2$ exhibits again the above-mentioned interplay between relativity and solvation for the relative stabilities of Au^{III} and Au^{I}

DOI: 10.1021/acs.inorgchem.5b01632
Inorg. Chem. 2015, 54, 9869−9875

Table 4. Reaction Energies, Enthalpies, and Gibbs Free Energies (in kJ mol^{-1}) for the $AuCl_4^-$ + OH^- ⇌ $AuCl_3OH^-$ + Cl^- and $AuCl_3OH^-$ ⇌ $AuClOH^{-2}$ + Cl_2 Reactions[a]

	nonrelativistic			relativistic		
reaction	ΔE	$\Delta G_{298\ K}$	$\Delta H_{298\ K}$	ΔE	$\Delta G_{298\ K}$	$\Delta H_{298\ K}$
			$AuCl_4^-$ + OH^- ⇌ $AuCl_3OH^-$ + Cl^-			
gas phase	−148.6	−133.4	−141.3	−158.6	−142.7	−150.6
COSMO	−84.8	−70.9	−78.4	−96.0	−81.3	−88.6
D-COSMO-RS	−65.4	−49.6	−59.0	−77.2	−62.6	−70.0
			$AuCl_3OH^-$ ⇌ $AuClOH^{-2}$ + Cl_2			
gas phase	115.3	65.1	109.6	187.6	137.8	182.1
COSMO	66.4	16.2	60.9	147.6	98.6	142.4
D-COSMO-RS	22.0	−30.6	16.1	127.6	78.1	122.4

[a]Comparison of gas-phase and aqueous solution results (with COSMO and D-COSMO-RS) at B3LYP level with Turbomole, using a nonrelativistic or scalar relativistic Au ECP, respectively.

Table 5. Reaction Energies, Enthalpies, and Gibbs Free Energies (in kJ mol^{-1}) for the Disproportionation Reaction 3 $AuCl_2^-$ ⇌ $AuCl_4^-$ + 2 $Au_{(s)}$ + 2 Cl^-[a]

	nonrelativistic			relativistic		
	ΔE	$\Delta G_{298\ K}$	$\Delta H_{298\ K}$	ΔE	$\Delta G_{298\ K}$	$\Delta H_{298\ K}$
gas phase	616.0	664.0	605.3	506.2	539.1	494.5
gas phase (+cohesive energy[b])	333.3	372.6	322.1	98.4	130.4	86.7
COSMO	192.1	236.2	181.2	−74.0	−42.0	−85.8
D-COSMO-RS	177.9	226.0	167.3	−161.5	−128.6	−173.2

[a]Comparison of gas-phase and aqueous solution results (with COSMO and D-COSMO-RS) at B3LYP level with Turbomole, using a nonrelativistic or scalar relativistic Au ECP, respectively. [b]Cohesive energy for solid gold from non- and scalar relativistic DFT calculations, respectively (see text), added to the gas-phase data.

species. Relativity strongly favors $AuCl_3OH^-$, solvation favors reduction, and the nonadditivity between the two influences (larger solvent destabilization at nonrelativistic level) leads to the largest relativistic stabilization at D-COSMO-RS level (108.7 kJ/mol). The overall results are consistent with an overall predominance of $AuCl_3OH^-$ in solution at neutral pH under the chosen ambient conditions, which clearly is a relativistic effect.

3.5. Disproportionation of $AuCl_2^-$. In the above-mentioned geochemical context, the disproportionation reaction 3 $AuCl_2^-$ ⇌ $AuCl_4^-$ + 2 $Au_{(s)}$ + 2 Cl^- is of fundamental interest, and Table 5 provides computational data in solution that are again closest to dilute solution at neutral pH and ambient temperature. While the gas-phase data would suggest the equilibrium to be clearly on the left side, the interplay between solvation/aggregation and relativity shifts it to the right side. Here, the cohesion energy of solid gold is obviously a major contributor. We have taken the nonrelativistic and scalar relativistic computed energies (219.0 and 333.8 kJ/mol, respectively) for it from the DFT-based work of ref 61 (local density approximation with mixed plane-wave and Gaussian basis sets, scalar- vs nonrelativistic norm-conserving pseudopotentials). The scalar-relativistic value agrees reasonably well with the experimental cohesive energy (367.6 kJ/mol). It is clear that relativity shifts the equilibrium strongly to the right (a) due to the enhanced cohesion energy of solid gold, but also (b) due to the stabilization of $AuCl_4^-$ relative to $AuCl_2^-$ (see above). Solvation does in this case also contribute to a more exergonic reaction (Table 5), due to the efficient solvation of the chloride ions.

4. CONCLUSIONS

Not unexpectedly, scalar relativistic effects stabilize Au^{III} halide complexes AuX_4^- (X = F, Cl, Br, I) in solution against reductive elimination of halogen. Due to a strong nonadditivity between relativistic and solvent effects, the relativistic stabilization of the higher oxidation state is enhanced in solution. The D-COSMO-RS model, which simulates implicitly the effects of hydrogen bonding between solute and solvent, thus also provides larger relativistic stabilizations. DFT methods were calibrated against CCSD(T) gas-phase calculations. B3LYP calculations with D-COSMO-RS indicate that in dilute aqueous solution at neutral pH and ambient conditions, the AuX_4^- complexes are stable with respect to halogen elimination, except for the iodide, which exhibits a slightly exergonic reaction at this level. Calculations at the same level indicate that under the same conditions, $AuCl_4^-$ is unstable against hydrolysis to $AuCl_3OH^-$, whereas the latter species in turn is redox-stable. Under these conditions, $AuCl_2^-$ would exergonically disproportionate. All of these computational data are consistent with the available experimental observations on speciation of gold halides in dilute aqueous solution at neutral pH and ambient temperature, and they clearly expose the large role of relativity.

Closer examination of the nonadditivity between relativity and solvent effects by analyses of NPA charges and surface charge densities has confirmed that the relativistic reduction of bond polarity, in particular for the Au^I halide complexes, diminishes solvent effects compared to nonrelativistic levels. This, in turn, leads to smaller solvent destabilization of the Au^{III} oxidation state.

■ ASSOCIATED CONTENT

Supporting Information

The Supporting Information is available free of charge on the ACS Publications website at DOI: 10.1021/acs.inorgchem.5b01632.

DOI: 10.1021/acs.inorgchem.5b01632
Inorg. Chem. 2015, 54, 9869−9875

Gold valence basis sets used in this work for all calculations. Spin−orbit contributions to total and reaction energies. Full citation of ref 19. (PDF)

AUTHOR INFORMATION

Corresponding Authors

*E-mail: hbs@chem.wayne.edu.
*E-mail: martin.kaupp@tu-berlin.de.
*E-mail: p.a.schwerdtfeger@massey.ac.nz.

Notes

The authors declare no competing financial interest.

ACKNOWLEDGMENTS

H.B.S. acknowledges support from the New Zealand Institute for Advanced Study (NZIAS). Work at TU Berlin has been supported by the DFG excellence cluster UniCat. H.B.S. and M.K. would like to thank P.S. for his hospitality and support during their visits to the NZIAS.

REFERENCES

(1) Pyykkö, P. *Annu. Rev. Phys. Chem.* **2012**, *63*, 45−64.
(2) Pyykkö, P. *Chem. Rev.* **1988**, *88*, 563−594.
(3) Iliaš, M.; Kellö, V.; Urban, M. *Acta Phys. Slov.* **2010**, *60*, 259−391.
(4) Pyykkö, P. *Angew. Chem., Int. Ed.* **2004**, *43*, 4412−4456.
(5) Pyykkö, P. *Inorg. Chim. Acta* **2005**, *358*, 4113−4130.
(6) Wang, X.; Andrews, L.; Riedel, S.; Kaupp, M. *Angew. Chem., Int. Ed.* **2007**, *46*, 8371−8375.
(7) Schwerdtfeger, P. *J. Am. Chem. Soc.* **1989**, *111*, 7261−7262.
(8) Schwerdtfeger, P.; Boyd, P. D. W.; Brienne, S.; Burrell, A. K. *Inorg. Chem.* **1992**, *31*, 3411−3422.
(9) Ahuja, R.; Blomqvist, A.; Larsson, P.; Pyykkö, P.; Zaleski-Ejgierd, P. *Phys. Rev. Lett.* **2011**, *106*, 018301.
(10) Schwerdtfeger, P.; Heath, G. A.; Dolg, M.; Bennett, M. A. *J. Am. Chem. Soc.* **1992**, *114*, 7518−7527.
(11) Seth, M.; Faegri, K.; Schwerdtfeger, P. *Angew. Chem., Int. Ed.* **1998**, *37*, 2493−2496.
(12) Kutzelnigg, W. *Angew. Chem., Int. Ed. Engl.* **1984**, *23*, 272−295.
(13) Kaupp, M.; von Schnering, H. G. *Angew. Chem., Int. Ed. Engl.* **1993**, *32*, 861−863.
(14) Kaupp, M.; Dolg, M.; Stoll, H.; von Schnering, H. G. *Inorg. Chem.* **1994**, *33*, 2122−2131.
(15) Seth, M.; Schwerdtfeger, P.; Dolg, M. *J. Chem. Phys.* **1997**, *106*, 3623−3632.
(16) Söhnel, T.; Brown, R.; Kloo, L.; Schwerdtfeger, P. *Chem. - Eur. J.* **2001**, *7*, 3167−3173.
(17) Puddephatt, R. J. *The Chemistry of Gold*; Elsevier: Amsterdam, 1978.
(18) Renz, M.; Kess, M.; Diedenhofen, M.; Klamt, A.; Kaupp, M. *J. Chem. Theory Comput.* **2012**, *8*, 4189−4203.
(19) Gaussian 09: Frisch, M. J. et al., Gaussian, Inc.: Wallingford, CT, 2009.
(20) Schwerdtfeger, P. *ChemPhysChem* **2011**, *12*, 3143−3155.
(21) Schwerdtfeger, P.; Dolg, M.; Schwarz, W. H. E.; Bowmaker, G. A.; Boyd, P. D. W. *J. Chem. Phys.* **1989**, *91*, 1762−1774.
(22) Figgen, D.; Rauhut, G.; Dolg, M.; Stoll, H. *Chem. Phys.* **2005**, *311*, 227−244.
(23) Peterson, K. A.; Figgen, D.; Goll, E.; Stoll, H.; Dolg, M. *J. Chem. Phys.* **2003**, *119*, 11113−11123.
(24) Becke, A. D. *J. Chem. Phys.* **1993**, *98*, 5648−5652.
(25) Schlöder, T.; Kaupp, M.; Riedel, S. *J. Am. Chem. Soc.* **2012**, *134*, 11977−11979.
(26) Gong, Y.; Zhou, M.; Kaupp, M.; Riedel, S. *Angew. Chem.* **2009**, *121*, 8019−8023.
(27) Riedel, S.; Kaupp, M. *Coord. Chem. Rev.* **2009**, *253*, 606−624.
(28) Wang, X.; Andrews, L.; Riedel, S.; Kaupp, M. *Angew. Chem.* **2007**, *119*, 8523−8527.
(29) Riedel, S.; Renz, M.; Kaupp, M. *Inorg. Chem.* **2007**, *46*, 5734−5738.
(30) Riedel, S.; Kaupp, M. *Inorg. Chem.* **2006**, *45*, 10497−10502.
(31) Riedel, S.; Kaupp, M. *Angew. Chem.* **2006**, *118*, 3791−3794.
(32) Riedel, S.; Kaupp, M. *Inorg. Chem.* **2006**, *45*, 1228−1234.
(33) Riedel, S.; Straka, M.; Kaupp, M. *Chem. - Eur. J.* **2005**, *11*, 2743−2755.
(34) Riedel, S.; Straka, M.; Kaupp, M. *Phys. Chem. Chem. Phys.* **2004**, *6*, 1122−1127.
(35) Yanai, T.; Tew, D.; Handy, N. *Chem. Phys. Lett.* **2004**, *393*, 51−57.
(36) Vydrov, O. A.; Scuseria, G. E.; Perdew, J. P. *J. Chem. Phys.* **2007**, *126*, 154109.
(37) Dunning, T. H., Jr. *J. Chem. Phys.* **1989**, *90*, 1007−1023.
(38) Woon, D. E.; Dunning, T. H., Jr. *J. Chem. Phys.* **1993**, *98*, 1358−1371.
(39) Ahlrichs, R.; Baer, M.; Haeser, M.; Horn, H.; Koelmel, C. *Chem. Phys. Lett.* **1989**, *162*, 165−169.
(40) Treutler, O.; Ahlrichs, R. *J. Chem. Phys.* **1995**, *102*, 346−354.
(41) TURBOMOLE V6.3 a development of University of Karlsruhe and Forschungszentrum Karlsruhe GmbH, 1989−2007, TURBOMOLE GmbH, since 2007; available from http://www.turbomole.com.
(42) Vosko, S. H.; Wilk, L.; Nusair, M. *Can. J. Phys.* **1980**, *58*, 1200−1211.
(43) Klamt, A. *J. Phys. Chem.* **1995**, *99*, 2224−2235.
(44) Sinnecker, S.; Rajendran, A.; Klamt, A.; Diedenhofen, M.; Neese, F. *J. Phys. Chem. A* **2006**, *110*, 2235−2245.
(45) Klamt, A. *WIRE Comput. Mol. Sci.* **2011**, *1*, 699−709.
(46) Eckert, F.; Klamt, A. *AIChE J.* **2002**, *48*, 369−385.
(47) Renz, M.; Kaupp, M. *J. Phys. Chem. A* **2012**, *116*, 10629−10637.
(48) Theilacker, K.; Buhrke, D.; Kaupp, M. *J. Chem. Theory Comput.* **2015**, *11*, 111−121.
(49) Eckert, F., Klamt, A. COSMOtherm, Version C2.1, Release 01.11; COSMOlogic GmbH & Co. KG: Leverkusen, Germany, 2010.
(50) Perdew, J. P. *Phys. Rev. B: Condens. Matter Mater. Phys.* **1986**, *33*, 8822−8824.
(51) Weigend, F.; Furche, F.; Ahlrichs, R. *J. Chem. Phys.* **2003**, *119*, 12753−12762.
(52) Weigend, F.; Baldes, A. *J. Chem. Phys.* **2010**, *133*, 174102.
(53) Weigend, F. *J. Comput. Chem.* **2008**, *29*, 167−175.
(54) Kaupp, M. *J. Comput. Chem.* **2007**, *28*, 320−325.
(55) Kaupp, M. In *Anorganische Chemie - Prinzipien von Struktur und Reaktivität*; 5th ed. Steudel, R., Ed.; de Gruyter: Berlin, 2014.
(56) Kaupp, M.; von Schnering, H. G. *Inorg. Chem.* **1994**, *33*, 4718−4722.
(57) Gammons, C. H.; Yu, Y.; Williams-Jones, A. E. *Geochim. Cosmochim. Acta* **1997**, *61*, 1971−1983.
(58) Pan, P.; Wood, S. A. *Geochim. Cosmochim. Acta* **1991**, *55*, 2365−2371.
(59) Peck, J. A.; Tait, C. D.; Swanson, B. I.; Brown, G. E., Jr *Geochim. Cosmochim. Acta* **1991**, *55*, 671−676.
(60) Farges, F.; Sharps, J. A.; Brown, G. E., Jr *Geochim. Cosmochim. Acta* **1993**, *57*, 1243−1252.
(61) Takeuchi, N.; Chan, C. T.; Ho, K. M. *Phys. Rev. B: Condens. Matter Mater. Phys.* **1989**, *40*, 1565−1570.

DOI: 10.1021/acs.inorgchem.5b01632
Inorg. Chem. 2015, 54, 9869−9875